

Supporting Information

Activation and Allosteric Modulation of Human μ Opioid Receptor in Molecular Dynamics

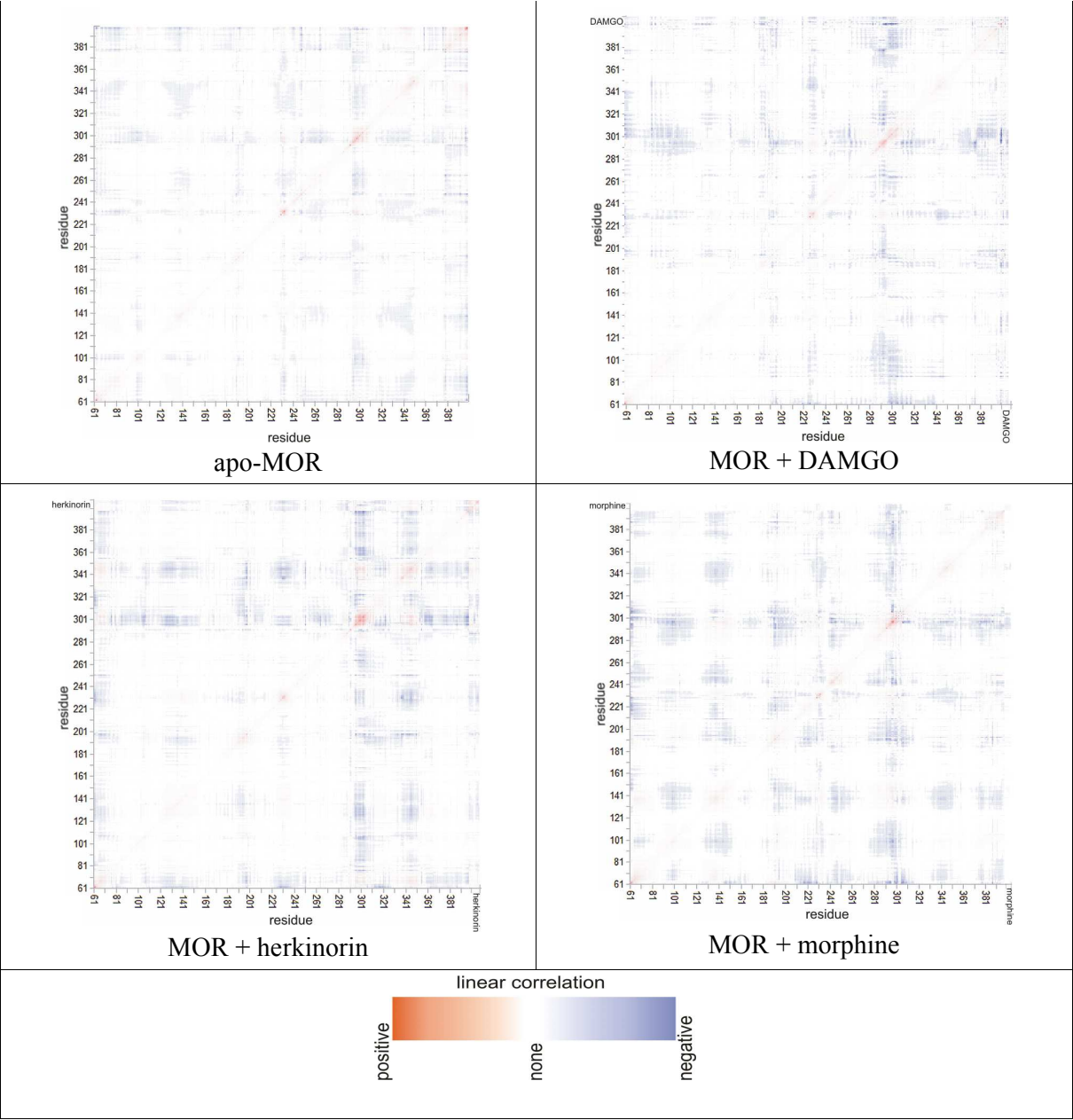
Damian Bartuzi¹, Agnieszka A. Kaczor^{1,2}, Dariusz Matosiuk¹

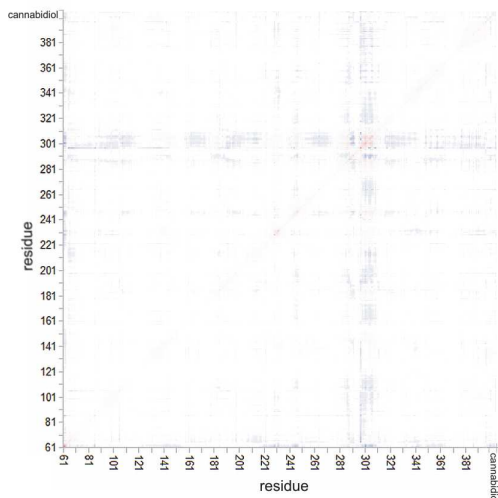
¹Department of Synthesis and Chemical Technology of Pharmaceutical Substances with Computer Modeling
Lab, Faculty of Pharmacy with Division of Medical Analytics, Medical University of Lublin, 4A Chodźki
St., PL-20093 Lublin, Poland, tel.: +48815357365; fax: +48815357366

²School of Pharmacy, University of Eastern Finland, Yliopistonranta 1, P.O. Box 1627, FI-70211 Kuopio,
Finland

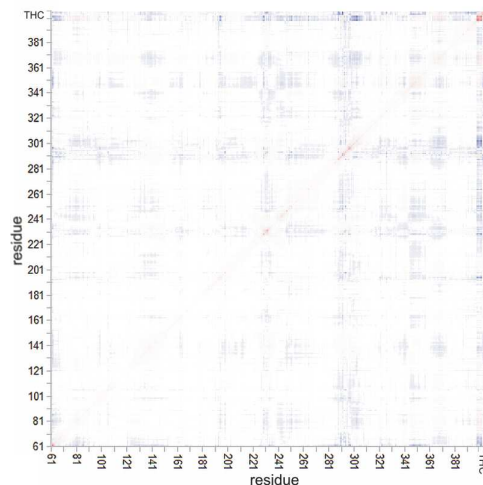
e-mail: damian.bartuzi@umlub.pl

Table S1. Covariance matrices for simulations of μ opioid receptor in complex with Gs protein with various ligands and allosteric modulators, performed in raft-like membrane. Modulator binding unharnesses linear correlations observed in agonist-bound receptor simulations, which is most pronounced in simulation of MOR+cannabidiol and MOR+DAMGO+Salvinorin A, but also evident in simulations MOR+THC, MOR+DAMGO+THC, MOR+DAMGO+cannabidiol.

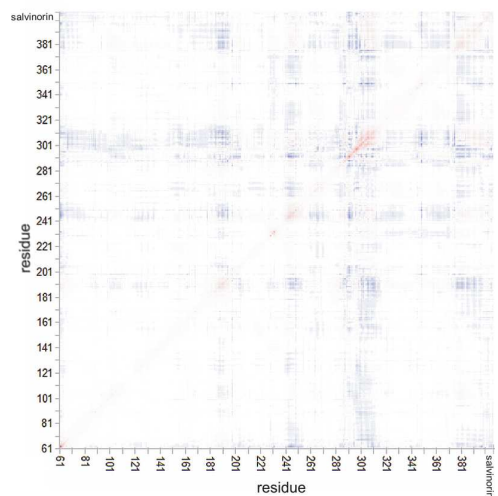




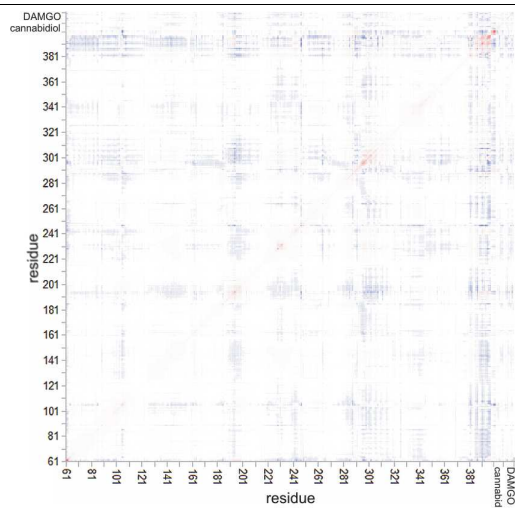
MOR + cannabidiol



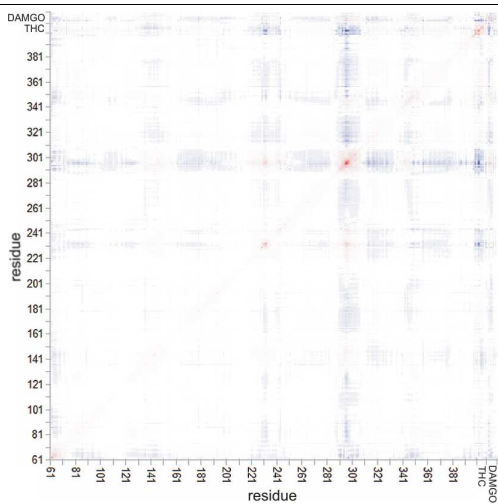
MOR + THC



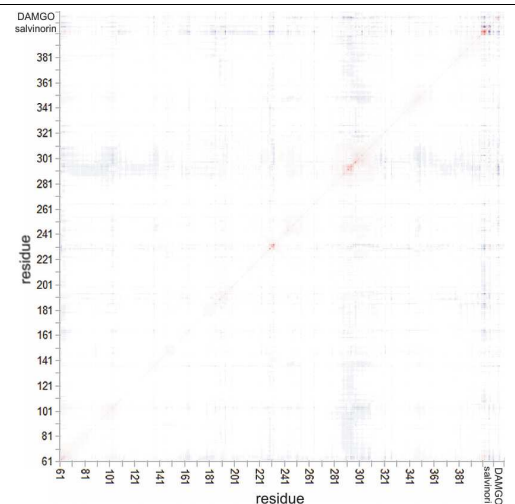
MOR + salvinorin A



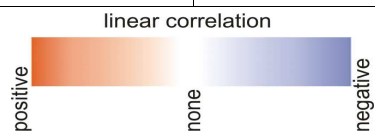
MOR + DAMGO + cannabidiol



MOR + DAMGO + THC



MOR + DAMGO + salvinorin A



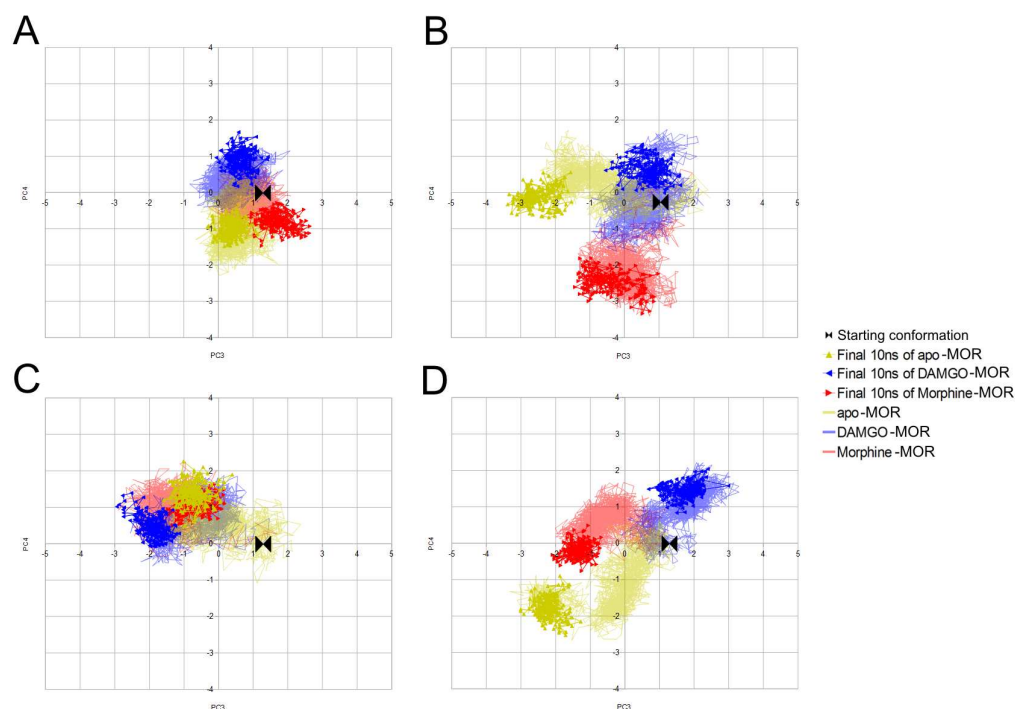


Figure S1. The third and the fourth principal components of morphine-MOR, DAMGO-MOR and the apo-MOR trajectories in four membranes in the common subspace. Plot presented in four parts for clarity. Main differences concern the pure POPC and 40% CHL membranes. A-raft-like membrane, B-POPC membrane, C- 20% CHL membrane, D – 40% CHL membrane.

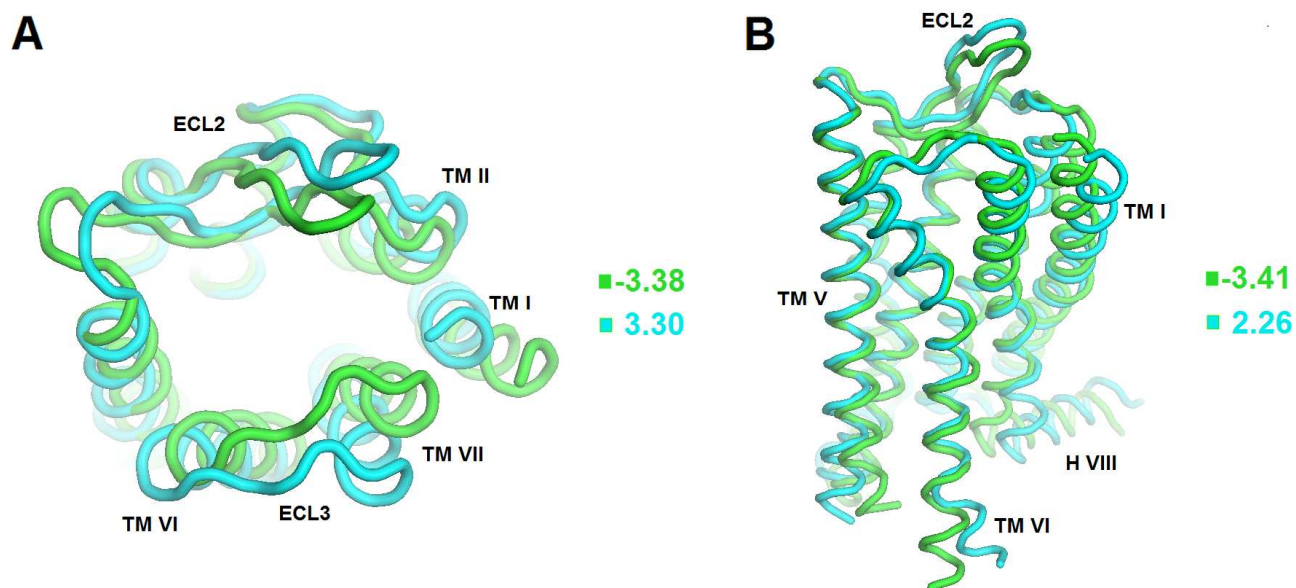


Figure S2. Trajectory projections on the average structure resulting from PCA of morphine-MOR, DAMGO-MOR and the apo-MOR trajectories in four membranes. Projections correspond to extreme values along the third (A) and the fourth (B) PC. The frames exaggerate occurring changes and do not show exact simulation snapshots. Legend corresponds to PC values from the Supplementary Figure 1. A – The PC3 contains mainly motions of the TM VII and the ECL2. B – The PC4 describes relative movement of the intracellular parts of TM V and TM VI, as well as some motions of the helix VIII and the ECL2.

Table S2. Averages and total drift of protein-modulator interaction energy values. Table refers to complexes in raft-like membrane.

Complex	Average Coulomb energy (kJ/mol)	Total Coul. Energy drift	Average VDW energy (kJ/mol)	Total VDW Energy drift
MOR+CDI	-33.08	5.26	-128.11	-4.06
MOR+THC	-17.55	3.93	-133.73	22.66
MOR+SAL	-30.91	17.32	-160.98	1.654
MOR+DAMGO+CDI	-38.12	-10.28	-120.87	-15.12
MOR+DAMGO+THC	-6.12	-4.07	-127.80	-19.05
MOR+DAMGO+SAL	-21.26	32.12	-135.90	55.41

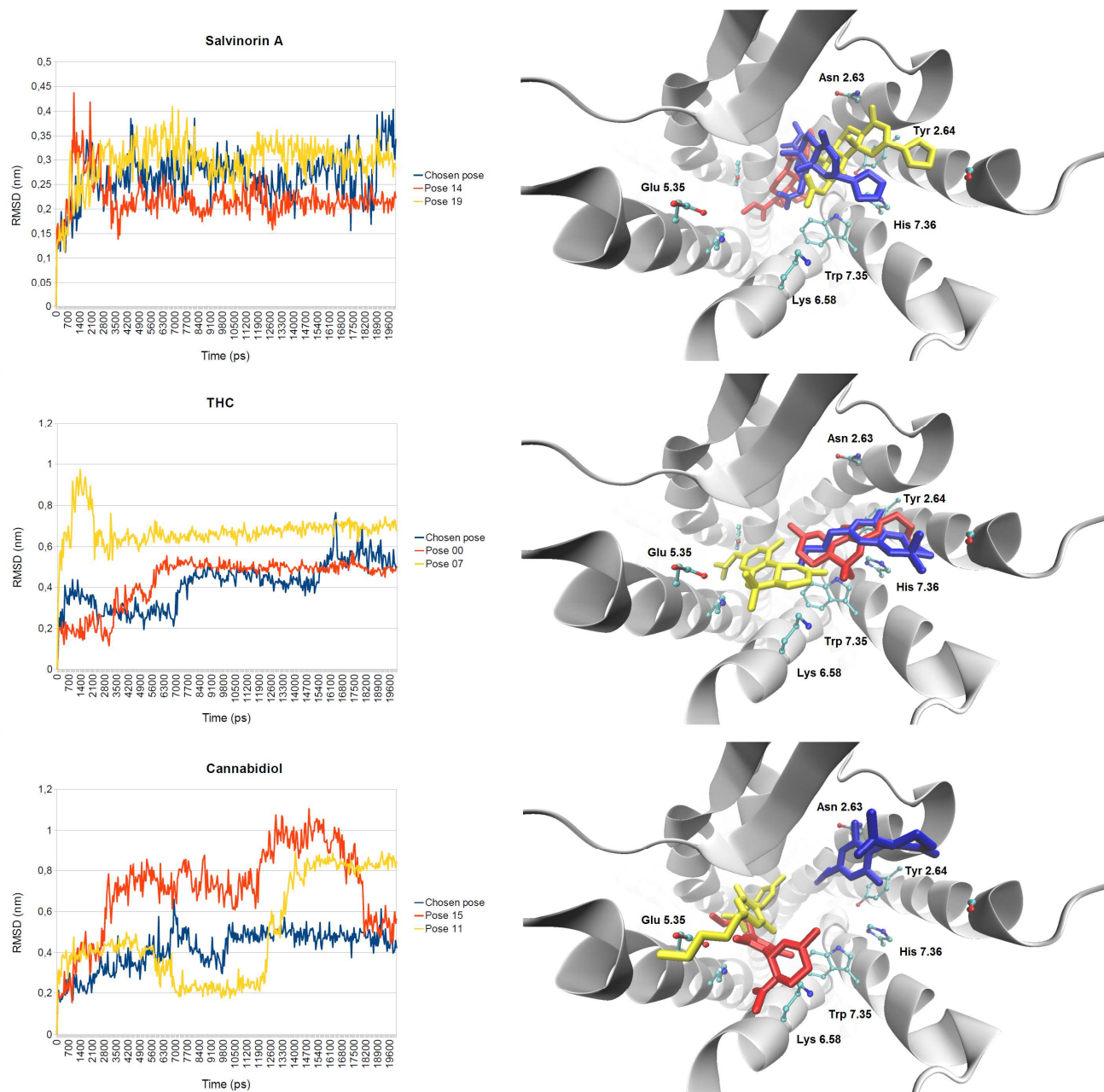


Figure S3. RMSD of the best docking poses of modulators during the initial 20 ns MD simulations.

Table S3. Number of different water molecules that occupied space within 5 Å from the conserved Asp 3.32 throughout simulations and their residence time. Table refers to complexes in raft-like membrane.

Ligands	DAMGO	DAMGO + CDI	DAMGO + THC	DAMGO + SAL
Very long-resident water molecules ($t > 10$ ns)	9	9	17	21
Long-resident water molecules (10 ns $> t > 1$ ns)	145	43	7	62
Medium-resident water molecules (100 ps $< t < 1$ ns)	271	153	26	90
Short-resident water molecules ($t < 100$ ps)	318	303	32	109
Total	743	508	82	282

Table S4. Number of different water molecules that occupied space within 5 Å from the conserved Asp 3.32 throughout simulations and their residence time. Table refers to complexes containing DAMGO and salvinorin A in different membranes.

Membrane	Raft-like		POPC		POPC + 20% CHL		POPC + 40% CHL	
Ligands	DAMGO	DAMGO+SAL	DAMGO	DAMGO+SAL	DAMGO	DAMGO+SAL	DAMGO	DAMGO+SAL
Very long-resident water molecules ($t > 10$ ns)	9	21	2	5	6	8	12	4
Long-resident water molecules (10 ns $> t > 1$ ns)	145	62	127	23	109	39	73	45
Medium-resident water molecules (100 ps $< t < 1$ ns)	271	90	283	31	126	242	300	93
Short-resident water molecules ($t < 100$ ps)	318	109	281	56	165	256	306	72
Total	743	508	693	115	406	498	691	214